AIAA JOURNAL
Vol. 36, No. 8, August 1998

Luminescent Oil-Film Skin-Friction Meter

Tianshu Liu* and J. P. Sullivan†
Purdue University, West Lafayette, Indiana 47906

The principles of a luminescent oil-film skin-friction meter are described. Unlike the interferometric oil-film methods, this technique measures skin friction by detecting luminescent intensity of an oil film seeded with luminescent probe molecules. The measurement system for luminescence imaging is simple and easy to use, and this technique requires no special surface. The feasibility of this method is examined by applying it to several typical flows.

Introduction

SKIN friction is one of the most important physical quantities in aerodynamics. For several decades, a variety of techniques have been developed for measurement of skin friction. Comprehensive reviews of the techniques of measurement of skin friction were given by Winter[1] and Settles.[2] Of many existing techniques, the oil-film skin-friction meter invented by Tanner and Blows[3] is particularly attractive because it does not depend on flow characteristics. Tanner and Blows studied the motion of an oil film on a surface in shear flow and first realized that skin friction can be determined by detecting temporal-spatial evolution of the thickness of a thin oil film. In their papers, a laser interferometer was used to measure the thickness of a thin oil film. The laser interferometer was further improved by Monson and Higuchi[4] and Kim and Settles.[5] The image-based global interferometer was developed by Monson et al.,[6] Naughton and Brown,[7] and Zilliac.[8] In addition to these interferometric methods, Bandyopadhyay and Weinstein[9] developed a reflection-type oil-film meter.

This paper describes a luminescent oil-film skin-friction meter and its application to several typical flows. This technique utilizes a luminescent oil and determines the rate of change of the thickness of the oil film by sensing its luminescent emission. Compared with the interferometers, this method simplifies instrumentation and eliminates the requirement of a special surface. Because the measurement system for luminescence is robust and easy to use, this technique can be applied to any model surface in various aerodynamic experiments including flight testing. It is noted that some researchers have used luminescent oils for visualization of boundary-layer transition and flow separation.[10,11]

Fundamentals of Luminescent Oil-Film Method

Local Dynamics of an Oil Film

Tanner and Blows[3] presented a control volume analysis of a thin oil film on a smooth surface subject to the action of shear stress. For a constant local shear stress, they obtained a simple relation between oil-film thickness h and skin friction τ:

$$\tau = \mu x/ht \tag{1}$$

where μ is the oil viscosity, t is the time from starting the flow, and x is the coordinate from the oil leading edge in the local shear stress direction. The formula (1) is commonly used as a fundamental relation for an oil-film skin-friction meter. In fact, Eq. (1) describes an intermediate asymptotic state of the evolution of an oil film, where shear stress is so dominant that other forces, such as pressure gradient, surface tension, and gravity, can be neglected.

The development of a two-dimensional oil droplet (film) subjected to a constant shear stress on a wall in gas flow is described by the generalized Landau–Levich equation (see Appendix A)

$$\frac{\partial h}{\partial t} = -\frac{\tau h}{\mu}\frac{\partial h}{\partial x} + \frac{1}{3\mu}\frac{\partial}{\partial x}\left(h^3\frac{\partial p_{\text{gas}}}{\partial x}\right) - \frac{\sigma}{\mu}\frac{\partial}{\partial x}\left(\frac{1}{3}h^3\frac{\partial^3 h}{\partial x^3}\right) \tag{2}$$

where σ is the surface tension and p_{gas} is the local pressure in gas flow. The first, second, and third terms on the right-hand side of Eq. (2) represent the contributions of shear stress, pressure gradient, and surface tension, respectively. Considering an intermediate asymptotic state in which the solution to Eq. (2) no longer depends on the initial and boundary conditions,[12] we obtain

$$\tau = \frac{\mu x}{ht} + h\frac{\partial p_{\text{gas}}}{\partial x} \tag{3}$$

Obviously, Eq. (1) is a special form of Eq. (3) when $h\partial p_{\text{gas}}/\partial x$ is neglected. In this study, we utilize another version of Eq. (1),

$$\tau = \mu\frac{\mathrm{d}}{\mathrm{d}t}\left(\frac{\mathrm{d}h}{\mathrm{d}x}\right)^{-1} \tag{4}$$

Because the formula (4) contains only the temporal and spatial derivatives of h, it avoids determining the error-introducing variables x (the distance to the oil leading edge) and t (the starting time).

Determination of Skin Friction by Detecting Luminescent Intensity

The oil-film skin-friction meters involve measurements of the oil-film thickness and its temporal and spatial derivatives. Instead of interferometers used in most of the previous studies, a luminescent oil-film system is used. A luminescent oil is made by adding luminescent probe molecules to silicone oil. Under excitation provided by an illumination source with a suitable wavelength λ_1, such as a ultraviolet (uv) lamp or a laser, the luminescent oil can emit radiation with a longer wavelength λ_2 due to the Stokes shift. Because the oil-film thickness is proportional to luminescent intensity when the film is thin, the film thickness can be measured by detecting luminescent intensity. Driscoll et al.[13] have measured liquid film thickness in an airblast fuel atomizer by laser-induced luminescence.

For a luminescent oil film on a wall, an analysis of radiation transfer from the oil film gives an expression for the integrated luminescent intensity $\langle I_{\lambda_2}\rangle$ across the oil film (see Appendix B):

$$\left\langle I_{\lambda_2}\right\rangle = I_0\eta\exp[-(\kappa_1+\kappa_2)h][F(h,\kappa_1+\kappa_2) + \rho_r F(h,\kappa_2-\kappa_1)] \tag{5}$$

where h is the oil-film thickness, η is a constant proportional to the quantum efficiency of the luminescent molecule, I_0 is the intensity of the incident excitation light, ρ_r is the reflectivity of the wall surface to the incident excitation light, and κ_1 and κ_2 are the absorption coefficients for the excitation light and luminescent light through the oil film, respectively. The function $F(\zeta, a)$ in Eq. (5) is given by $F(\zeta, a) = a^{-1}[\exp(a\zeta) - 1]$. Here the luminescent intensity is defined as radiative energy transferred per unit time, solid angle,

Received July 15, 1997; revision received Dec. 8, 1997; accepted for publication March 16, 1998.

*Postdoctoral Research Assistant, School of Aeronautics and Astronautics; currently Research Scientist, High Technology Corporation, 28 Research Drive, Hampton, VA 23666. Member AIAA.

†Professor, School of Aeronautics and Astronautics. Member AIAA.

spectral variable, and area normal to the ray. When $h \ll 1$, Eq. (5) becomes

$$\langle I_{\lambda_2} \rangle = I_0 \eta (1 + \rho_r) h + o(h) \tag{6}$$

Substitution of Eq. (6) into Eq. (4) yields

$$\tau = C \frac{\mathrm{d}}{\mathrm{d}t} \left(\frac{\mathrm{d}I}{\mathrm{d}x} \right)^{-1} + \varepsilon \approx C \frac{1}{\Delta t} \left(\frac{\Delta x}{\Delta I} \right) + \varepsilon \tag{7}$$

where I denotes $\langle I_{\lambda_2} \rangle$ in a simplified notation and C is defined as $C = \mu I_0 \eta (1 + \rho_r)$. The formula (7) is an operational form of calibration relation for a luminescent oil-film skin-friction meter. The coefficient C depends on the illumination intensity, physical properties of the luminescent oil, and surface scattering properties. In general, ε is a small quantity of $\mathcal{O}(h)$. When h is small enough and ε can be neglected, Eq. (7) is simply $\tau = C\beta$, where β is defined as $\beta = \mathrm{d}/\mathrm{d}t(\mathrm{d}I/\mathrm{d}x)^{-1}$. In the data reduction, the linear regression is used to calculate $(\Delta x/\Delta I)/\Delta t$.

In principle, the luminescent intensity I can be calibrated a priori as a function of h, and therefore the absolute value of skin friction can be calculated using the formula (4). However, the a priori calibration requires other independent techniques for measuring h. In practice, the in situ method is used as a convenient alternative, which determines the coefficients C and ε in Eq. (7) by using known skin-friction data at two reference locations. The reference data are provided by other techniques such as the Preston-tube and laser interferometer skin-friction meter. Once C and ε are given, the skin-friction distribution can be calculated from luminescent intensity images. In particular, for $\varepsilon \approx 0$, the absolute skin friction needs to be known at only one reference location to obtain the skin-friction distribution.

Measurement System

Luminescent Oil

To make a luminescent oil, 0.2 g of powder of europium thenoyltrifluoroacetonate (EuTTA, Kodak) is dissolved into 1 ml of dope thinner (AeroGloss, Pactra, Inc.). Next, the dope thinner containing EuTTA is mixed with 20 ml of Dow Corning 200 silicone oil with 200-cS viscosity. After the solvent dope thinner evaporates in a short time, EuTTA molecules are homogeneously distributed in the silicone oil. The resulting luminescent oil, a nearly clear fluid in the absence of excitation, emits red radiation at 612 nm when illuminated by a uv lamp. EuTTA is chosen as a luminescent material because it has a high quantum efficiency. In this study, the temperature sensitivity of EuTTA is not a concern in low-speed flows with a constant temperature. In fact, the temperature effect on luminescence can partially offset the temperature effect on oil viscosity.

Photodetector System

The charge-coupled device (CCD) camera system for a luminescent oil film is similar to that used for temperature- and pressure-sensitive paints.[14,15] Figure 1 shows the measurement system for a luminescent oil film. A luminescent oil film applied to a surface is excited by a light source with a suitable wavelength. The luminescent intensity images of the oil film captured by the camera are optically filtered to eliminate illumination light. The images are recorded on tape and are later digitized with a frame grabber board for data processing. The temporal-spatial development of the oil film can be studied by analyzing the successive images because the oil-film thickness is proportional to the luminescent intensity. With this information, skin friction can be calculated. The measurement system used here includes an eight-bit standard CCD camera for imaging and uv lamps for illumination.

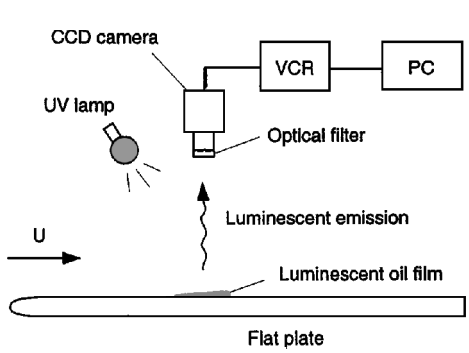

Fig. 1 CCD camera system for a luminescent oil film.

Accuracy

The accuracy of a luminescent oil-film skin-friction meter depends on various error sources. The elemental error sources in an oil-film interferometer skin-friction meter have been studied by Zilliac[8] and Naughton and Brown.[16] Many of these error sources also contribute to the uncertainty associated with the luminescent oil-film skin-friction meter. The rss procedure for Eq. (7) gives the relative uncertainty of skin friction

$$\frac{U_\tau^2}{\tau^2} = \frac{U_c^2}{C^2} + \frac{U_{\Delta t}^2}{(\Delta t)^2} + \frac{U_{\Delta x}^2}{(\Delta x)^2} + \frac{U_{\Delta I}^2}{(\Delta I)^2} + \frac{U_{\mathrm{DR}}^2}{\tau^2} \tag{8}$$

where U_X/X denotes the relative uncertainty of the measured variable X and U_{DR}/τ is the relative uncertainty in the data reduction. Without loss of generality, the variable ε in Eq. (7) is neglected in Eq. (8). The uncertainty U includes the bias error B and the precision error P ($U^2 = B^2 + P^2$). The error sources can be classified into three categories: calibration, data acquisition, and data reduction. The following sections will discuss the errors in Eq. (8) and estimate the upper limit of the total uncertainty.

Calibration Errors

The term U_c/C in Eq. (8) represents the calibration error in determination of the coefficient C. In the a priori calibration, this term includes the uncertainties in measuring the oil viscosity and calibrating the luminescent intensity as a function of the oil-film thickness. In the in situ calibration, this term is simply the relative uncertainty of the technique used for measurements of skin friction at reference locations. For example, when a Preston tube is utilized in the in situ calibration, U_c/C is the uncertainty associated with the Preston-tube method.

Data-Acquisition Errors

The terms $U_{\Delta t}/\Delta t$, $U_{\Delta x}/\Delta x$, and $U_{\Delta I}/\Delta I$ in Eq. (8) belong in the data-acquisition errors. The first two terms, $U_{\Delta t}/\Delta t$ and $U_{\Delta x}/\Delta x$, are directly related to the temporal and spatial resolutions of the CCD camera, whereas $U_{\Delta I}/\Delta I$ contains the contributions from many error sources in luminescent intensity measurement. The quantities Δt and Δx represent the characteristic scales in time and space for the development of an oil film. The temporal scale Δt may vary from seconds to minutes, depending on the magnitudes of skin friction and oil viscosity. In the data reduction, a good linear regression requires a certain number of data points in appropriately large Δt and Δx. Therefore, there are the minimum temporal scale $(\Delta t)_{\min}$ and spatial scale $(\Delta x)_{\min}$ for the linear regression. Typical values are $(\Delta t)_{\min} = 10$ s and $(\Delta x)_{\min} = 10$ pixels for a standard CCD camera system with the time resolution of 0.033 s and spatial resolution of 512×480 pixels. In this case, $U_{\Delta t}/\Delta t$ is 0.33% and $U_{\Delta x}/\Delta x$ is 10%.

The term $U_{\Delta I}/\Delta I$ represents the relative uncertainty in the luminescent intensity measurement with a CCD camera. Uncertainty estimates for the luminescent paint intensity measurement with CCD cameras have been discussed by Morris et al.[17] and Cattafesta and Moore.[18] The error sources include the random illumination fluctuation (P), systematic illumination drift (B), nonuniform illumination (B), shot noise (P), preamplifier noise (P), dark current (P), CCD nonlinearity (B), digitizer bias (B), ambient light (B), and optical leaking of camera filter (B), where B and P indicate the bias and precision errors, respectively. The precision errors can be reduced by averaging sequential frames of images in a short duration. Based on the uncertainty estimates for an eight-bit standard CCD camera,[18] we obtain an estimate $U_{\Delta I}/\Delta I = 9.2\%$ for $\Delta I = 50$ in a full intensity range of 256 after 30 frames of images are averaged to reduce the random errors. In contrast, a 14-bit, scientific-grade CCD camera has much smaller uncertainty $U_{\Delta I}/\Delta I = 1.4\%$ in the same conditions.

Generally, the luminescent intensity measurement is shot noise limited.

The nonuniform illumination and temperature dependence of luminescence also contribute to $U_{\Delta I}/\Delta I$. The effect of the nonuniform illumination can be corrected by taking the ratio between the luminescent emissions from the oil film and reference luminescent indicators with a different emission wavelength. This is similar to the two-color luminophore method for temperature- and pressure-sensitive paints.[14] Temperature affects both the oil viscosity and luminescence. The temperature dependence of the oil viscosity is described by $\mu(T) = \mu(T_{\text{ref}}) \exp[-C_\mu(T - T_{\text{ref}})]$, where T_{ref} is the reference temperature. The temperature dependence of the luminescent intensity has a similar expression, $I(T) = I(T_{\text{ref}}) \exp[-C_I(T - T_{\text{ref}})]$, in a certain temperature range. Interestingly, the temperature effects on the oil viscosity and luminescence partially cancel. Usually, the temperature effects are not considered when the relative skin friction is calculated in isothermal conditions.

Data-Reduction Errors

The term U_{DR}/τ is mainly associated with the validity of the formula (1) that is the intermediate asymptotic solution of Eq. (2). The intermediate asymptotic state may be reached in a region between the oil leading and trailing edges after an onset period. Clearly, the effects of the pressure gradient, shear gradient, and surface tension are ignored in Eq. (1). Zilliac[8] has estimated the errors due to neglecting the pressure and shear gradients. The pressure gradient causes 0.14% change of skin friction. The shear gradient leads to the uncertainty ranging from 0 to 20%. The surface tension term is a higher-order small quantity, and its effect is appreciable only at the oil leading and trailing edges. A more complicated phenomenon is the surface wave on the oil film.[19] In our experiments, the surface wave is indeed observed in a short period of seconds after the wind tunnel starts. Because the surface wave disappears quickly as the oil film thins, it does not affect the data reduction.

Total Uncertainty

Considering the aforementioned major error sources, we give the upper limit of the total uncertainty in the worst case for a standard CCD camera system:

$$U_\tau^2/\tau^2 < \left(U_c^2/C^2\right)_{\max} + (0.24)^2 \tag{9}$$

The large uncertainty bound in Eq. (9) is attributed to not only the poor spatial resolution and low signal-to-noise ratio of a standard CCD camera but also the simple data-reduction model (1) that neglects the shear gradient and other effects. The accuracy can be significantly improved using a scientific-grade CCD camera for imaging and completely solving the thin-oil-film differential equation for data reduction.

In addition, the repeatability in luminescent oil-film skin-friction measurements can be estimated by repetition tests in a flat plate turbulent boundary layer. The repeatability reflects the uncertainty associated with the random errors. Figure 2 shows a histogram of measurements compared with the Gaussian distribution. The data are collected in the repetition tests over several days in a skin-friction range from 0.15 to 0.7 N/m^2. The standard deviation is 0.028 N/m^2, and the mean repeatability is about 7%.

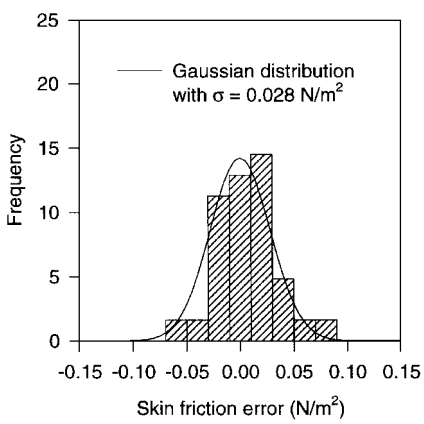

Fig. 2 Histogram of measurements in a flat plate turbulent boundary layer.

Experiments

Oil Wedge

To examine the relation between the oil thickness and luminescent intensity, an oil wedge test was devised. As shown in Fig. 3, a simple setup has a thin glass plate inclined with respect to the wall using a razor to form an oil wedge. In general, the virtual leading edge of the oil wedge is not located at the lower end of the glass plate. The virtual leading edge should be determined by extrapolating the linear portion of the luminescent intensity distribution. Figure 4 shows typical results for the luminescent Dow Corning 200 silicone oil on white Mylar® and aluminum surfaces. A curvefit to the experimental data using Eq. (5) is also shown in Fig. 4. The luminescent intensity distributions exhibit a linear behavior with the oil thickness for $h < 90\ \mu$m.

Turbulent Boundary Layer on a Flat Plate

The turbulent boundary layer on a flat plate serves as a canonical flow to examine the feasibility of the luminescent oil-film skin-friction meter. Experiments are carried out in a blowdown low-speed wind tunnel with a 0.46 × 0.3 m test section at Purdue University. The Plexiglas® flat plate has a 1:6 elliptical nose and a 12.7-mm thickness. A 3.2-mm-thick and 73-mm-wide aluminum plate is flush mounted at the centerline on the plate. A roughness band and a 1.6-mm-diam round rod are placed near the leading edge of the plate to trip the boundary layer. The measured velocity profiles in the boundary layer shown in Fig. 5 exhibit the log-law form at 0.4 m from the plate leading edge for several different freestream velocities. This indicates that the tripped boundary layer is fully turbulent at this location. A luminescent oil droplet of about 5-mm diam is placed at this location on the aluminum surface, and a Preston tube is also installed at the same streamwise location for reference skin-friction measurement. The calibration formula given by Patel[20] is used for the Preston-tube measurement.

The temporal-spatial evolution of the luminescent oil droplet is detected by a CCD camera. Figure 6 shows a developing sequence of luminescent intensity distributions of the oil droplet on the plate subject to a shear stress of 0.49 N/m^2. Because the luminescent intensity I is proportional to the oil-film thickness h, Fig. 6 depicts the three-dimensional geometric evolution of the oil droplet in the flat plate turbulent boundary layer. After the wind tunnel starts, a

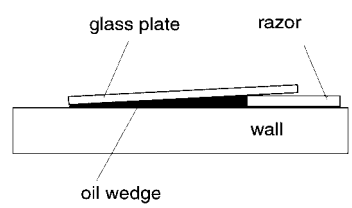

Fig. 3 Oil wedge setup.

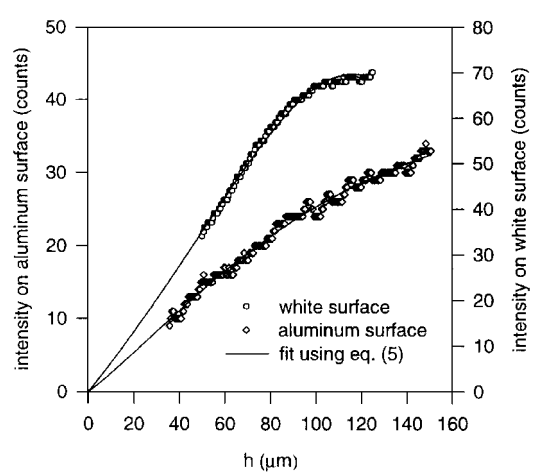

Fig. 4 Relation between oil thickness and luminescent intensity.

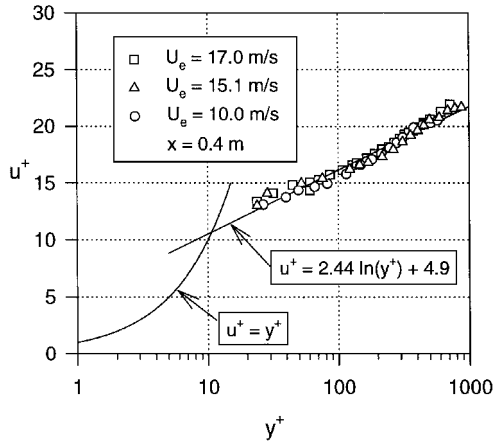

Fig. 5 Velocity profiles at 0.4 m from the leading edge in a tripped flat plate turbulent boundary layer.

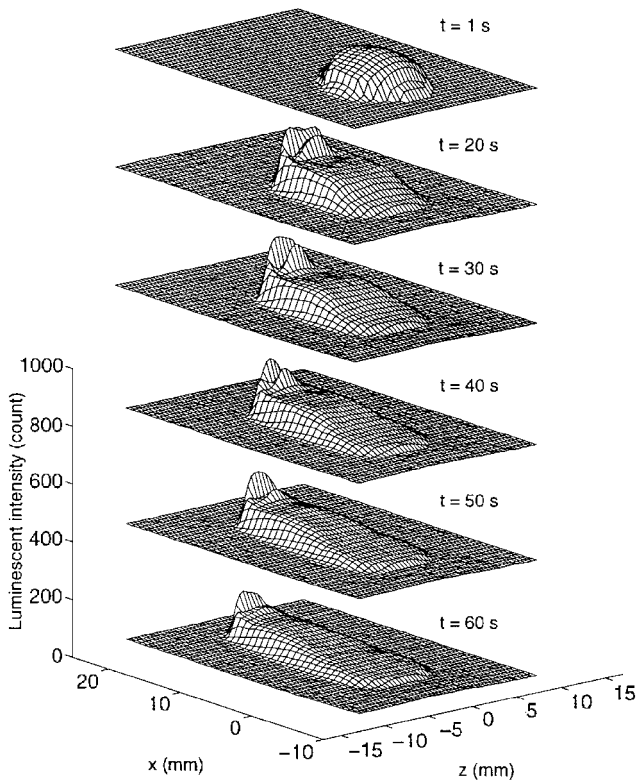

Fig. 6 Evolution of an oil droplet in a flat plate turbulent boundary layer under the action of shear stress of 0.49 N/m^2. The luminescent intensity is proportional to the oil-film thickness.

wedge forms near the oil leading edge, whose angle decreases as time increases. An oil crest near the moving trailing edge appears as a result of oil accumulation. Figure 7 shows the corresponding luminescent intensity profiles at the centerline of the oil droplet. It is found that the intensity profiles are linear only in a limited region. The nonlinear behavior is attributed to a fact that the intermediate asymptotic state is not completely achieved in the whole domain of the oil droplet. However, the linear relationship between I and x is approximately valid in the region immediately after the oil leading edge. In this region, the gradient $\mathrm{d}I/\mathrm{d}x$ can be evaluated using the linear regression. Figure 8 shows $(\mathrm{d}I/\mathrm{d}x)^{-1}$ as a linear function of t for different values of skin friction. Using the linear regression again, we calculate the rate of change of the reciprocal luminescent intensity gradient $\beta = \mathrm{d}/\mathrm{d}t(\mathrm{d}I/\mathrm{d}x)^{-1}$. Figure 9 shows $\beta = \mathrm{d}/\mathrm{d}t(\mathrm{d}I/\mathrm{d}x)^{-1}$ as a function of skin friction, where the absolute values of skin friction are obtained using a Preston tube. The data in Fig. 9 verify the fundamental relation (7). The boundary layer is assumed to be fully turbulent from the plate leading

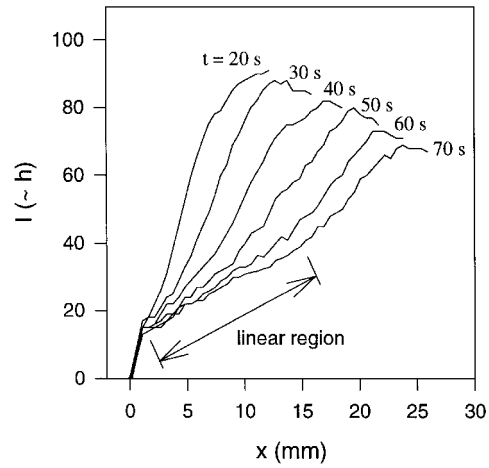

Fig. 7 Luminescent intensity profiles at the centerline of an oil droplet at different times under the action of shear stress of 0.49 N/m^2.

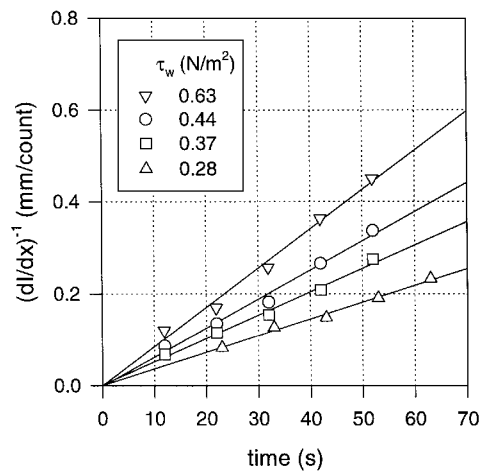

Fig. 8 Reciprocal luminescent intensity gradient as a function of time for different values of skin friction.

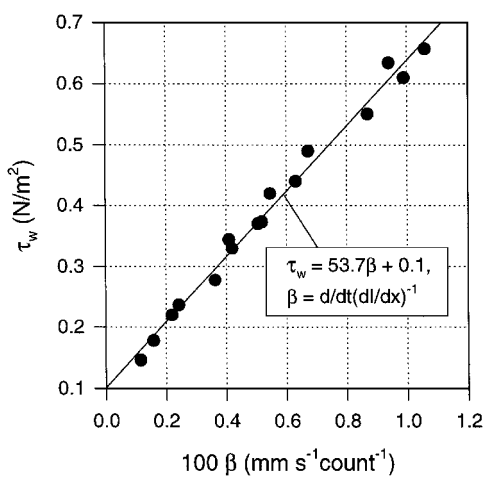

Fig. 9 $\beta = \mathrm{d}/\mathrm{d}t(\mathrm{d}I/\mathrm{d}x)^{-1}$ as a function of skin friction.

edge due to the tripping. The skin-friction coefficients calculated for different Reynolds numbers are plotted in Fig. 10 against two empirical correlations given by Prandtl and Nikuradse (see Ref. 21). The measured data fall between these correlations. In Fig. 10, Re_x is the Reynolds number based on the distance x from the plate leading edge. Considering the estimates of the elemental errors, we give the total uncertainty of 12% for the measurements of skin friction in the flat plate turbulent boundary layer.

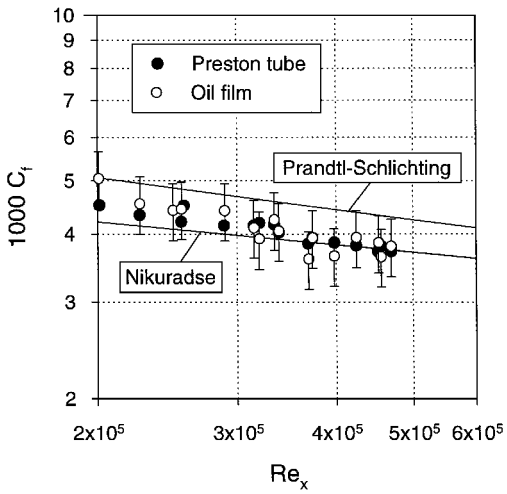

Fig. 10 Skin-friction coefficient on a flat plate as a function of the Reynolds number based on the distance from the plate leading edge. The boundary layer is assumed to be fully turbulent from the leading edge.

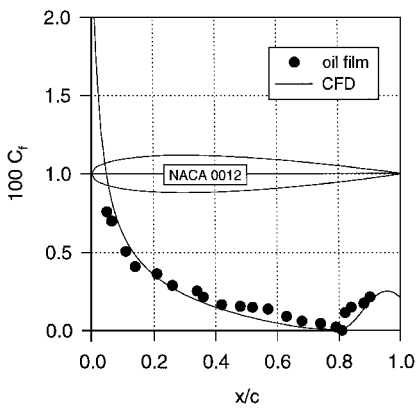

Fig. 11 Chordwise distribution of skin friction on a NACA 0012 airfoil model for $Re_c = 2.4 \times 10^5$ at zero angle of attack.

NACA Airfoils

Skin-friction measurements at low Reynolds numbers are made on NACA 0012 and NACA 65_4-021 airfoil sections. The NACA 0012 airfoil with a 0.2-m chord is made of aluminum. The Styrofoam® NACA 65_4-021 airfoil with a 0.15-m chord is covered by aluminum foil on its surface. Experiments are made in the same low-speed wind tunnel used for the flat plate tests. Before the wind tunnel starts, an oblique oil strip is brushed on the surface across the airfoil. After the flow is started, the development of the luminescent oil strip, which is dominated by local shear stress, is detected by a CCD camera. The aforementioned data reduction procedure is used to obtain $\beta = \mathrm{d}/\mathrm{d}t(\mathrm{d}I/\mathrm{d}x)^{-1}$, which is proportional to skin friction. In the in situ calibration to determine the coefficients C and ε in Eq. (7), a computational fluid dynamics code XFOIL for the analysis of subsonic airfoils is used, which can provide good prediction for skin friction at least in a laminar boundary layer on an airfoil.[22] As long as reliable skin-friction data are given at a number of reference locations ($\geq$2) in the laminar region, the chordwise skin-friction distribution on the whole airfoil can be obtained. Figures 11 and 12 show the chordwise distributions of skin-friction coefficient on the NACA 0012 airfoil for $Re_c = 2.4 \times 10^5$ and on the NACA 65_4-021 airfoil for $Re_c = 1.7 \times 10^5$ at zero angle of attack, respectively, where Re_c is the Reynolds number based on the chord of the airfoil section. The in situ calibrations for Figs. 11 and 12 are made in the laminar region from $x/c = 0.1$–0.35. Observed boundary-layer transition occurs approximately at $x/c = 0.8$ for both airfoils, which is consistent with the computations. The measured skin-friction distribution also indicates a small separation bubble before transition on the NACA 65_4-021 airfoil.

Skin-friction measurements for higher Reynolds numbers are made on a wooden NACA 66_3-418 airfoil section with a 0.508-m chord in the Boeing/Purdue subsonic wind tunnel with a 4×6 ft closed test section. The surface of the airfoil is covered by a white Mylar sheet whose scattering properties enhance the luminescence detected by a camera. Figure 13 shows the chordwise skin-friction distribution on the upper surface of the airfoil for $Re_c = 9.6 \times 10^5$ at zero angle of attack.

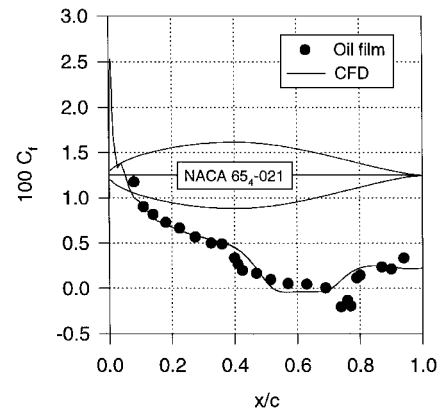

Fig. 12 Chordwise distribution of skin friction on a NACA 65_4-021 airfoil model for $Re_c = 1.7 \times 10^5$ at zero angle of attack.

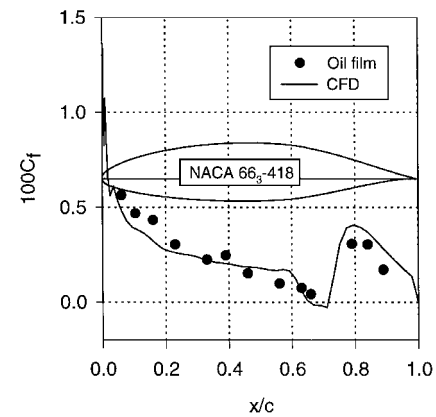

Fig. 13 Chordwise distribution of skin friction on the upper surface of a NACA 66_3-418 airfoil model for $Re_c = 9.6 \times 10^5$ at zero angle of attack.

Conclusions

A luminescent oil-film skin-friction meter measures skin friction by sensing the temporal-spatial development of luminescent intensity of an oil film. A luminescent oil, Dow Corning silicone oil with EuTTA probe molecules, is utilized. A standard CCD camera is used for detecting the luminescent emission from an oil film illuminated by uv lamps. The measurement system is robust and easy to use and does not require a special surface. This technique can provide relative values of skin friction without a priori calibration. The capability of this instrument has been demonstrated in measurements of skin friction in a flat plate turbulent boundary layer and flows over three NACA airfoils for different Reynolds numbers.

Appendix A: Oil-Film Equation

Consider a two-dimensional oil film on a wall in gas flow under the action of a constant shear stress when the gravity effect is neglected. The streamwise velocity u in the thin oil film is

$$u = \frac{y}{\mu}\left[\tau - \frac{\mathrm{d}p_{\mathrm{oil}}}{\mathrm{d}x}\left(h - \frac{1}{2}y\right)\right] \tag{A1}$$

where y is the coordinate normal to the wall, h is the oil film thickness, p_{oil} is the pressure in the oil film, μ is the oil viscosity, and τ is the shear stress exerted on the film. The continuity equation gives the normal velocity v at the oil–gas interface:

$$v(y = h) = \frac{h^3}{3\mu}\frac{\mathrm{d}^2 p_{\mathrm{oil}}}{\mathrm{d}x^2} + \frac{h^2}{2\mu}\frac{\mathrm{d}p_{\mathrm{oil}}}{\mathrm{d}x}\frac{\mathrm{d}h}{\mathrm{d}x} \tag{A2}$$

On the oil–gas interface $y = h$, a free-surface condition is $v = h_t + uh_x$, and a force balance in the normal direction is $-[p] + [\mu \boldsymbol{S} \cdot \boldsymbol{n} \cdot \boldsymbol{n}] = \sigma h_{xx}(1 + h_x^2)^{-3/2}$, where [ ] denotes the jump across the oil–gas interface, $\mu \boldsymbol{S}$ is the viscous stress tensor, $\boldsymbol{n}$ is the unit normal vector of the interface, and σ is the surface tension. When $[\mu \boldsymbol{S} \cdot \boldsymbol{n} \cdot \boldsymbol{n}] \ll 1$ and $h_x^2 \ll 1$ are assumed for a thin oil film, the force balance becomes $[p] = p_{\text{oil}} - p_{\text{gas}} \approx -\sigma h_{xx}$. Substitution of Eqs. (A1) and (A2) and the force balance relation into the free-surface condition yields Eq. (2), which can reduce to the Landau–Levich equation in the absence of the shear stress and pressure gradient.

Appendix B: Radiation from a Luminescent Oil Film

Radiation from a luminescent oil film on a surface involves two major processes. The first process is absorption of an excitation light through the oil film. The second is luminescent radiation, which is an absorbing-emitting process in the oil film. Luminescent intensity emitted from the oil film in one direction can be determined based on the transport equations of radiative energy.

Consider an oil film with a thickness h on a wall. An incident excitation light beam with a wavelength λ_1 enters the oil film in the normal direction $\boldsymbol{n}$ to the wall. Without scattering and other sources for radiative energy, the incident light will be attenuated by absorption through the oil medium. The intensity attenuation of the incident excitation light with λ_1 through an infinitesimal element $\mathrm{d}y$ can be described by $\mathrm{d}I_{\lambda_1} = -\kappa_I I_{\lambda_1} \mathrm{d}y$, where κ_1 is the absorption coefficient of the oil medium for the incident excitation light with λ_1, I_{λ_1} is the intensity of the excitation light, and the direction of the y coordinate is from the wall to the oil film. Here, the intensity is defined as radiative energy transferred per unit time, solid angle, spectral variable, and area normal to the ray. The boundary condition for I_{λ_1} is $I_{\lambda_1}(y = h) = I_0$, where I_0 is the intensity of the incident excitation light before entering the oil film. The solution for I_{λ_1} is $(I_{\lambda_1})_{\text{incident}} = I_0 \exp[-\kappa_1(h - y)]$. This relation describes the decay of the incident excitation light intensity through the oil film. When the incident excitation light impinges on the wall surface, the light reflects in the direction $-\boldsymbol{n}$. The reflected excitation light is also attenuated by absorption. The intensity of the reflected light is $(I_{\lambda_1})_{\text{reflected}} = \rho_r I_0 \exp[-\kappa_1(h + y)]$, where ρ_r is the reflectivity of the wall material to the excitation light. Thus, the total intensity of the excitation light in the oil film is

$$I_{\lambda_1}(y) = I_0 \exp[-\kappa_1(h - y)] + \rho_r I_0 \exp[-\kappa_1(h + y)] \tag{B1}$$

After the luminescent probe molecules in the oil film absorb the energy from the excitation light with a wavelength λ_1, they emit luminescence with a longer wavelength λ_2 due to the Stokes shift. Luminescent transfer in the oil film is an absorbing-emitting process. The change of the luminescent intensity I_{λ_2} in an infinitesimal element $\mathrm{d}y$ can be described by

$$\mathrm{d}I_{\lambda_2} = -\kappa_2 I_{\lambda_2} \mathrm{d}y + S_{\lambda_2} \mathrm{d}y \tag{B2}$$

where κ_2 is the absorption coefficient of the oil medium for the luminescent light with λ_2. The luminescent source function is defined as $S_{\lambda_2} = \eta I_{\lambda_1}(y)$, where η is a constant proportional to the quantum efficiency of a probe molecule and $I_{\lambda_1}(y)$ is the intensity of the excitation light in the oil film. Because there is no luminescent emission at the wall, the boundary condition for Eq. (B2) is $I_{\lambda_2}(0) = 0$. The solution to Eq. (B2) is

$$I_{\lambda_2} = I_0 \eta \exp[-(\kappa_1 h + \kappa_2 y)][F(y, \kappa_1 + \kappa_2) + \rho_r F(y, \kappa_2 - \kappa_1)] \tag{B3}$$

where $F(\zeta, a)$ is defined as $F(\zeta, a) = a^{-1}[\exp(a\zeta) - 1]$. The luminescent intensity integrated from all infinitesimal elements across the oil film is

$$\langle I_{\lambda_2} \rangle = \int \mathrm{d}I_{\lambda_2} = I_0 \eta \exp[-(\kappa_1 + \kappa_2)h] \times [F(h, \kappa_1 + \kappa_2) + \rho_r F(h, \kappa_2 - \kappa_1)] \tag{B4}$$

Acknowledgments

The authors would like to thank Qiao Wu for his useful suggestions on radiation from a luminescent oil film. We are also thankful to three reviewers for their constructive comments.

References

[1] Winter, K. G., "An Outline of the Techniques Available for Measurement of Skin Friction in Turbulent Boundary Layer," *Progress in the Aerospace Sciences*, Vol. 18, No. 1, 1977, pp. 1–57.

[2] Settles, G. S., "Recent Skin Friction Techniques for Compressible Flows," AIAA Paper 86-1099, May 1986.

[3] Tanner, L. H., and Blows, L. G., "A Study of the Motion of Oil Films on Surfaces in Air Flow, with Application to the Measurement of Skin Friction," *Journal of Physics E: Scientific Instruments*, Vol. 9, No. 3, 1976, pp. 194–202.

[4] Monson, D. J., and Higuchi, H., "Skin Friction Measurements by a Dual-Laser-Beam Interferometer Technique," *AIAA Journal*, Vol. 19, No. 6, 1981, pp. 739–744.

[5] Kim, K. S., and Settles, G. S., "Skin Friction Measurements by Laser Interferometry in Swept Shock/Boundary-Layer Interactions," *AIAA Journal*, Vol. 28, No. 1, 1990, pp. 133–139.

[6] Monson, D. J., Mateer, G. G., and Menter, F. R., "Boundary-Layer and Global Skin Friction Measurement with an Oil-Fringe Imaging Technique," Society of Automotive Engineers, SAE Paper 932550, Costa Mesa, CA, Sept. 1993.

[7] Naughton, J. W., and Brown, J. L., "Surface Interferometric Skin-Friction Measurement Technique," AIAA Paper 96-2183, June 1996.

[8] Zilliac, G. G., "Further Development of the Fringe-Imaging Skin Friction Technique," NASA TM-110425, Dec. 1996.

[9] Bandyopadhyay, P. R., and Weinstein, L. M., "A Reflection-Type Oil-Film Skin-Friction Meter," *Experiments in Fluids*, Vol. 11, No. 5, 1991, pp. 281–292.

[10] Stalder, J. R., "The Use of Luminescent Lacquer for the Visual Indication of Boundary-Layer Transition," NACA TN-2263, Jan. 1951.

[11] Loving, D. L., and Katzoff, S., "The Fluorescent-Oil Film Method and Other Techniques for Boundary-Layer Flow Visualization," NASA Memo 3-17-59L, March 1959.

[12] Barenblatt, G. I., *Similarity, Self-Similarity, and Intermediate Asymptotics*, Consultants Bureau, New York, 1979, pp. 1–13.

[13] Driscoll, D. I., Schmitt, R. L., and Stevenson, W. H., "Thin Flowing Liquid Film Thickness Measurement by Laser Induced Fluorescence," *Journal of Fluids Engineering*, Vol. 114, March 1992, pp. 107–112.

[14] Liu, T., Campbell, B. T., Burns, S. P., and Sullivan, J. P., "Temperature- and Pressure-Sensitive Luminescent Paints in Aerodynamics," *Applied Mechanics Reviews*, Vol. 50, No. 4, 1997, pp. 227–246.

[15] McLachlan, B. G., and Bell, J. H., "Pressure-Sensitive Paint in Aerodynamic Testing," *Experimental Thermal and Fluid Science*, Vol. 10, No. 4, 1995, pp. 470–485.

[16] Naughton, J. W., and Brown, J. L., "Uncertainty Analysis for Oil-Film Interferometric Skin-Friction Measurement Techniques," American Society of Mechanical Engineers, ASME Paper FEDSM97-3475, Vancouver, BC, Canada, June 1997.

[17] Morris, M. J., Benne, M. E., Crites, R. C., and Donovan, J. F., "Aerodynamic Measurements Based on Photoluminescence," AIAA Paper 93-0175, Jan. 1993.

[18] Cattafesta, L. N., III, and Moore, J. G., "Uncertainty Estimates for Luminescent Temperature-Sensitive Paint Intensity Measurements," AIAA Paper 95-2193, June 1995.

[19] Murphy, J. D., and Westphal, R. V., "The Laser Interferometer Skin-Friction Meter: A Numerical and Experimental Study," *Journal of Physics E: Scientific Instruments*, Vol. 19, No. 9, 1986, pp. 744–751.

[20] Patel, V. C., "Calibration of the Preston Tube and Limitations on Its Use in Pressure Gradients," *Journal of Fluid Mechanics*, Vol. 23, No. 1, 1965, pp. 185–208.

[21] Schlichting, H., *Boundary-Layer Theory*, McGraw–Hill, New York, 1979, pp. 641–644.

[22] Drela, M., "XFOIL: An Analysis and Design System for Low Reynolds Number Airfoil," *Conference on Low Reynolds Number Airfoil Aerodynamics* (Univ. of Notre Dame), Springer–Verlag, New York, 1989.

G. Laufer
Associate Editor